Nuclear Instruments and Methods in Physics Research B 107 (1996) 67–70

ELSEVIER

NIM B
Beam Interactions with Materials & Atoms

ETACHA: a program for calculating charge states at GANIL energies

J.P. Rozet [a,*], C. Stéphan [b], D. Vernhet [a]

[a] GPS, Universités Paris 7 and Paris 6, (URA CNRS 017), 2 place Jussieu, 75251 Paris Cedex 05, France
[b] IPN, Université Paris Sud, BP N°1, 91405 Orsay Cedex, France

Abstract

A computer program calculating charge state distributions of ions with up to 28 electrons distributed over $n = 1$, 2 and 3 subshells has been developed. The model is based on an independent electron model taking into account electron loss, capture and excitation from and to all the subshells. Calculated atomic cross sections are recomputed periodically to take into account their dependence with the projectile energy and its mean charge state when they vary as a function of target thickness.

1. Introduction

Numerous studies have been devoted to measurement and prediction of charge state distributions of ions inside and outside solid targets. Indeed, these distributions are necessary not only in connection with the study of energy loss in matter [1], but also for the design and operation of heavy ion accelerator. Moreover, design and/or analysis of many atomic or nuclear physics experiments are based on a good knowledge of such distributions. Whereas it has been long considered that only equilibrium charge state distributions were needed (and could be predicted by semi-empirical models), non-equilibrium ones are now also desired [2]. Correspondingly, more sophisticated models have to be developed.

Calculation of charge state distributions is usually performed by solving a set of differential ("rate") equations which can be written

$$\frac{dY_i(x)}{dx} = \sum_j Y_j(x)\,\sigma_{ji} - Y_i(x) \sum_j \sigma_{ij} \qquad (1)$$

where $Y_i(x)$ denotes a fraction of ions in a specific state (with $\sum_i Y_i(x) = 1$), x the traversed target thickness and σ_{ij} stands for a collision cross section (or transition rate) from state i to state j.

In early models [3], the fractions $Y_i(x)$ were associated with a specific charge state. Then the cross sections σ_{ij} only correspond to charge-changing processes (electron gain or loss). However, it was soon recognized that excited state effects may play an important role in determining the charge state of ions in solid targets [3–5] (compared to gaseous ones). Indeed, ionization cross sections, for instance, increase rapidly with principal quantum number, leading to higher "effective" electron loss cross sections in excited ions compared to ground state ones of the same ionic charge. It is then more appropriate to calculate the fraction of ions in a specific configuration, where the number of electrons in each substate is taken into account. This means however that an infinite number of states should be considered: in practice, one has always to limit the number of excited states in the calculation. Since, when the principal quantum number, n, increases, electron loss cross sections increase and electron gain ones decrease, populations in excited states are expected to become negligible above some given n value. The maximum number of states to be considered can be chosen on physical grounds: for highly stripped relativistic light ions, Anholt [6] used a four-state model where only bare and one electron ion in 1s, 2s and 2p substates are considered. For heavier ions, Anholt and Meyerhof [6] used an eleven-state model including ions with 0, 1 or 2 electrons in 1s, 2s and 2p subshells. For lower velocities, it may be necessary to take into account large fractions of ions bearing many electrons: Betz et al. [8] used a model including ions with up to seven electrons distributed over 20 states, and where excited states with $n \geq 4$ are considered. In a previous model [9], we used as a starting point the calculation of the individual populations in 1s, 2s and 2p substates: the final charge state fractions, corresponding to ions with up to ten electrons, were calculated subsequently by combining these populations. Comparison with experiment shows that such a model gives satisfactory results for all the major components in the charge state distribution at large enough target thicknesses. However,

* Corresponding author. Tel. +33 1 44 27 7307, fax +33 1 44 27 7309, e-mail: rozet@gps.jussieu.fr.

SSDI 0168-583X(95)00800-4

new measurements, where thin targets (carbon foil with a target thickness of approximately 20 $\mu g/cm^2$) have been used and minor components (with a relative population of approximately 0.1%) have been determined, show disagreement with the model. We describe here a new version of our model which includes improvement on many features.

2. Cross sections

Several processes must be taken into account to predict the dynamical evolution of individual subshell populations:

– Non-radiative capture (NRC) cross sections can be accurately calculated within the continuum distorted wave approximation (CDW) [10]. Such calculations, however, require large computing time. We then use here the Eikonal approximation as suggested by Meyerhof et al. [11]. We have found in most cases their predictions to agree well enough with CDW ones for the present purpose. Radiative electron capture (REC) cross sections are calculated using the Bethe–Salpeter formula [12]. NRC and REC cross section calculations both apply to fully stripped ions where final hydrogenic wave functions can be used. For non fully stripped ions, we make use of the independent electron approximation whereby cross sections in a specific substate are proportional to the number of available vacancies [9]. Moreover, effective (screened) nuclear charges are used, further reducing cross sections. Capture cross sections up to $n = 3$ are considered.

– Ionization cross sections corresponding to 1s, 2s, 2p, 3s, 3p and 3d subshells are calculated in the plane–wave Born approximation [13,14] using screened hydrogenic wave functions for the initial and final states of atomic electrons. Screening and antiscreening effects by target electrons are also taken into account [6]. Such calculations are known to overestimate cross sections for intermediate velocity collisions and /or large target atomic numbers [2,15]. Calculated PWBA cross sections are corrected using a semi-empirical scaling law which has been found to give an overall satisfactory agreement with available experimental results or more sophisticated calculations [2,15]. We also make use here of the independent electron approximation which assumes the ionization cross sections to be proportional to the number of electrons in a specific subshell.

– Excitation cross sections are calculated in the same way as ionization ones. In the independent electron approximation, they are proportional to both the number of electrons in the initial state and the number of available vacancy in the final state. Calculated cross sections include direct and inverse intershell processes from and to all subshells in $n = 1$, 2, 3 and 4 shells as well as intrashell ("l mixing") 2s–2p, 3s–3p and 3p–3d ones. Excitation cross sections to $n \geq 4$ have been estimated from $n = 4$ ones, using a $1/n^3$ scaling law, and added to the ionization cross sections of initial states.

– Partial and total radiative and Auger decay rates in one electron ions or singly ionized atoms are available in the literature [12,16]. A scaling procedure due to Larkins [17] has previously been used successfully to account for a variation of excited states decay rates with the number of available electrons or vacancies in K, L and M shells [9,18]. This procedure has been used here to calculate radiative and KLL, KLM, KMM and LMM Auger decay rates.

3. Rate equations

Our model is limited to ions with up to 28 electrons, which can be distributed over the 1s, 2s, 2p, 3s, 3p and 3d subshells. Denoting n_1, n_2, n_3,n_4, n_5 and n_6 the number of electrons in each of these subshells, the number of possible configurations is equal to $3 \times 3 \times 7 \times 3 \times 7 \times 11 = 14553$. Besides, consideration of angular momentum and spin couplings would lead to a number of states orders of magnitude larger, prohibiting any feasible calculations to be attempted. Clearly, any unnecessary refinement has to be discarded in the model.

We first note that ionization and, in a first approximation, capture processes are spin independent, whereas excitation and decay processes may greatly differ between various coupled states of a given configuration (for instance, 1s2p ^{1}P and 1s2p ^{3}P states have very different lifetimes). Ionization and capture processes may be expected to populate statistically such states, and such a statistical population to be kept in the following. However, some departure from this picture, originating in the exclusion principle, must be considered: for instance, $1s^2$ state is a singlet one, and excitation from this state to 1s2p mainly populates $^1P_1$ state. Nevertheless, overall transition rates between various configurations through capture, ionization and excitation processes remain unaffected, and only mean decay rates, as calculated using our scaling procedure, may be somewhat inadequate. A careful study of possible consequences of neglecting such effects has been performed previously [9], and led to the conclusion that very small differences could be expected for this purpose.

In its present form, our model is based on a further approximation which reduces the number of calculated fractions from 14553 to 84: specific configurations are considered only for electrons in 1s, 2s and 2p states ($3 \times 3 \times 7 = 63$ configurations), and for $n = 3$ electrons, we only calculate the fraction of ions with a given population in 3s, 3p and 3d states ($3 + 7 + 11 = 21$ fractions). The 63 "correlated" fractions $Y_{KL}(n_1,n_2,n_3)$ of ions in a configuration $1s^{n1}2s^{n2}2p^{n3}$ are eventually combined to the 21 "uncorrelated" fractions $Y_{3s}(n_4)$, $Y_{3p}(n_5)$ and $Y_{3d}(n_6)$.

The fraction of ions of charge Q for a projectile of atomic number Z_p is then given by:

$$P(Q) = \sum_{\substack{n_1+n_2+n_3+n_4\\+n_5+n_6=Z_p-Q}} Y_{KL}(n_1,n_2,n_3)Y_{3s}(n_4)\,Y_{3p}(n_5)\,Y_{3d}(n_6). \quad (2)$$

The 63 correlated fractions $Y_{KL}(n_1, n_2, n_3)$ are solutions of a set of 63 differential equations which can be written

$$\frac{dY_{KL}(n_1n_2n_3)}{dx} = \sum_{n'_1\,n'_2\,n'_3} Y_{KL}(n'_1\,n'_2\,n'_3) \times \sigma\left(n'_1\,n'_2\,n'_3\bar{n}_4\,\bar{n}_5\,\bar{n}_6 \to n_1\,n_2\,n_3\,\bar{n}_4\,\bar{n}_5\,\bar{n}_6\right) - Y_{KL}(n_1\,n_2\,n_3)\sum_{n_1\,n_2\,n_3}\sigma\left(n_1\,n_2\,n_3\,\bar{n}_4\,\bar{n}_5\,\bar{n}_6 \to n'_1\,n'_2\,n'_3\,\bar{n}_4\,\bar{n}_5\,\bar{n}_6\right) \quad (3)$$

and the 21 uncorrelated fractions are solutions of a set of 21 differential equations written as

$$\frac{dY_{3s}(n_4)}{dx} = \sum_{n'_4} Y_{3s}(n'_4)\sigma\left(\bar{n}_1\,\bar{n}_2\,\bar{n}_3\,n'_4\,\bar{n}_5\,\bar{n}_6 \to \bar{n}_1\,\bar{n}_2\,\bar{n}_3\,n_4\,\bar{n}_5\,\bar{n}_6\right) - Y_{3s}(n_4)\sum_{n_4}\sigma\left(\bar{n}_1\,\bar{n}_2\,\bar{n}_3\,n_4\,\bar{n}_5\,\bar{n}_6 \to \bar{n}_1\,\bar{n}_2\,\bar{n}_3\,n'_4\,\bar{n}_5\,\bar{n}_6\right) \quad (4)$$

and similar equations for Y_{3p} and Y_{3d}.

The $\bar{n}_i$ are the mean number of electrons in a subshell, defined as

$$\bar{n}_{1s}(x) = \sum_{n_1,\,n_2,\,n_3} n_1\,Y_{KL}(n_1,\,n_2,\,n_3) \quad (5)$$

and similarly for $\bar{n}_{2s}$ and $\bar{n}_{2p}$, and

$$\bar{n}_{3s}(x) = \sum_{n_4} n_4\,Y_{3s}(n_4) \quad (6)$$

and similarly for $\bar{n}_{3p}$ and $\bar{n}_{3d}$.

4. Program

Microsoft Fortran version 5.0 has been used, producing an MS-DOS executable file which can be run on any PC with a Math processor, sufficient disk space and RAM, and proper memory settings.

Typical computing times are of a few minutes. On input, the user must enter the projectile atomic number, mass number, charge and velocity, the target atomic number, mass number and density. An optional input for energy loss corrections is provided: two tabulated values must be entered (stopping power is not calculated, only interpolated). The program then calculates capture cross sections into substates of fully stripped ions and ionization and excitation cross sections of hydrogen-like ions and these can be compared easily with other (possibly more sophisticated) calculations if available. At this point, the user can enter its own values for the cross sections, resulting in correcting factors which will be kept in the following.

The such obtained set of cross sections is then recalculated, using screening constants appropriate to the number of electrons in the incoming ion. Altogether, 38 cross sections are calculated. Addition of REC and NRC on one hand and of excitation to $n \geq 4$ shells to ionization on the other hand reduces this number to 26. At this point, nine radiative and Auger rates are also calculated.

The set of 84 differential equations is solved numerically using a predictor–corrector method [19]. Note that cross sections are functions of target thickness through the mean numbers of electrons which are (re-) calculated at each integration step. At each of these steps, also, the mean charge state of ion, defined by

$$\bar{Q} = \sum_{Q} Q\,P(Q) \quad (7)$$

is evaluated, as well as the actual energy E of the projectile if energy loss corrections are needed. When $\bar{Q}$ or E changes by more than a few percent, all cross sections are recalculated with the appropriate new screening constants, and integration starts again with a new set of cross sections and decay rates.

Finally, at each output thickness, autoionization outside the foil of each configuration is calculated, and the configurations combined according to Eq. (2) to produce output.

5. Results and discussion

The model predictions are in good agreement with experimental measurements performed at GANIL at the exit of the first cyclotron (medium energy line) or the exit of the second one, corresponding to projectile energies in the range 10–80 MeV/u. Improvements obtained with our new model when compared with the previous one [9] are illustrated in Fig. 1, where charge state distributions recorded for 13.6 MeV/u Ar^{17+} ions in carbon targets of well known thickness and purity are compared with both models. Clearly, the (small) fractions of Ar^{15+} ions at small target thicknesses are much better reproduced. We have also been able to measure [2] the fraction of metastable Ar^{16+} $1s2s\ ^3S_1$ ions produced by stripping of Ar^{10+} ions of the same velocity at the exit of a 107 $\mu g/cm^2$ carbon foil. For this target thickness, our model predicts a fraction

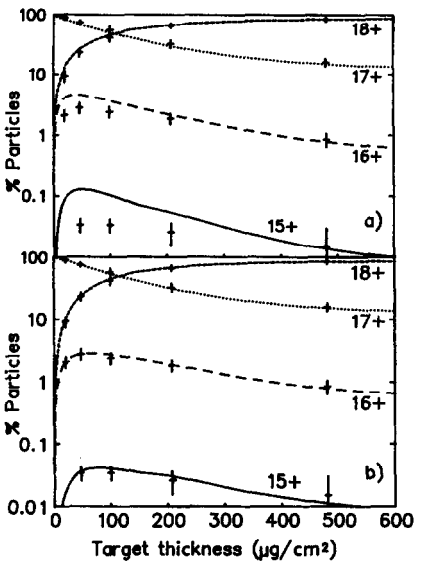

Fig. 1. Charge state distribution predictions compared to experiment for 13.6 MeV/u Ar^{17+} ion in carbon. (a) previous model [9]: (b) new ETACHA model.

of 4.3% of $^3S_1$ metastable states, in very good agreement with the measured value of (4.8 ± 1)%. Such a result supports strongly our assumption of a statistical population of coupled states for a given configuration (see discussion at the beginning of Section 3.)

6. Conclusion

Atomic cross sections may at present be calculated with good accuracy in the medium to high velocity collision regime, allowing reliable ab initio prediction of charge state distributions. However, the validity of such calculations at lower velocities or for heavier collision partners is not warranted. More extensive use of our code should help to better define its range of validity in the future.

Acknowledgements

The assistance and support of the technical staff of GANIL is gratefully acknowledged. The authors also wish to thank J. Kemmler and A. Cassimi for assistance in charge state measurements.

References

[1] F. Hubert, R. Bimbot and H. Gauvin, At. Data and Nucl. Data Tables 46 (1990)
[2] L. Adoui et al. / Nucl. Instr. and Meth. B 98 (1995) 312.
[3] See e.g. H.D. Betz, Rev. Mod. Phys. 44 (1972) 465.
[4] N. Bohr and J. Lindhardt, K. Dan. Vidensk. Selsk. Mat. Fys. Medd. 28 (7) (1954).
[5] H.D. Betz and L. Grodzins, Phys. Rev. Lett. 25 (1970) 211.
[6] R. Anholt, Phys. Rev. A 31 (1985) 3579.
[7] R. Anholt, and W.E. Meyerhof, Phys. Rev. A 33 (1986) 1556.
[8] H.D. Betz, R. Höpler, R. Schramm and W. Oswald, Nucl. Instr. and Meth. B 33 (1988) 185.
[9] J.P. Rozet, A. Chetioui, P. Piquemal, D. Vernhet, K. Wohrer, C. Stéphan and L. Tassan-Got, J. Phys. B 22 (1989) 33.
[10] Dž. Belkić, R. Gayet and A. Salin, Comput. Phys. Commun. 32 (1984) 385.
[11] W.E. Meyerhof, R. Anholt, J. Eichler, H. Gould, Ch. Munger, J. Alonso, P. Thieberger and H.E. Wegner, Phys. Rev. A 32 (1985) 3291.
[12] H.A. Bethe and E.E. Salpeter, Quantum Mechanics of One and Two-Electron Atoms (Academic Press, New York, 1957).
[13] G.S. Khandelwahl, B.H. Choi and E. Merzbacher, At. Data 1 (1969) 103.
[14] B.H. Choi, Phys. Rev. A 7 (1973) 2056.
[15] D. Vernhet, J.P. Rozet, K. Wohrer, L. Adoui, C. Stéphan, A. Cassimi and J.M. Ramillon, these Proceedings (SHIM'95), Nucl. Instr. and Meth. B 107 (1995) 71.
[16] M.O. Krause, J. Phys. Chem. Ref. Data 8 (1979) 307.
[17] F.P. Larkins, J. Phys. B 14 (1971) 229.
[18] J.P. Rozet and A. Chetioui, J. Phys. B 14 (1981) 73.
[19] D. Kahaner, C. Moler and S. Nash, Numerical Methods and Software (Prentice-Hall, 1988).